pp 1380–1407. © The Author(s), 2021. Published by Cambridge University Press on behalf of Royal Aeronautical Society.
doi:10.1017/aer.2021.23

Three-dimensional guidance and control for ground moving target tracking by a quadrotor

M. Sepehri Movafegh
Graduated from Control and Intelligent Systems Department
School of Electrical and Computer Engineering
University of Tehran
Tehran
Iran

S.M.M. Dehghan
smmd@mut.ac.ir
Faculty of Electrical and Computer Engineering
Malek Ashtar University of Technology
Tehran
Iran

R. Zardashti
Faculty of Aerospace
Malek Ashtar University of Technology
Tehran
Iran

ABSTRACT

This paper develops a three-dimensional guidance and control algorithm to ensure that a manoeuverable target is preserved by a quadrotor in a long-term tracking scenario. The proposed guidance approach determines the desired altitude of the quadrotor to adjust the field of view (FOV) to the union of two desired trusted and critical regions. The dimensions of the desired trusted region depend on the controller performance that is evaluated by the distance of the target from the center of the FOV. The critical region is a predefined margin around the trusted region that is defined by the operator based on the upper bounds of the quadrotor and target localisation errors. It also depends on the duration and magnitude of the temporal increase in the target velocity compared to the quadrotor velocity. A sufficient condition is provided for the minimum desired altitude of the quadrotor to ensure that the target is maintained in the FOV. Furthermore, a model predictive control (MPC) is employed to preserve

Received 14 March 2020; revised 14 February 2021; accepted 8 March 2021.

the target at the center of the aerial image and the desired altitude determined by the guidance law. Also, the integrals of the position errors are used to achieve null steady-state errors in the presence of wind disturbances. The simulation results show the effectiveness of the proposed approach in preserving the manoeuverable target in the FOV in the presence of the wind, the uncertainty of the target and quadrotor localisation, accelerations estimation errors, and terrain altitude variation.

Keywords: Quadrotor; 3D guidance and control law; Ground moving target tracking; Model predictive control (MPC)

NOMENCLATURE

GMT	Ground Moving Target
UAV	Unmanned Aerial Vehicle
MPC	Model Predictive Control
FOV	Field of View
LQR	Linear Quadratic Programing
UGV	Unmanned Ground Vehicle
ϕ, θ, ψ	Rotational Variables of Quadrotor
a_ϕ, a_θ, a_ψ	Rotational Acceleration of Quadrotor
w_ϕ, w_θ, w_ψ	Rotational Disturbance
x, y, z	Actual Translational Variables of Quadrotor
$\hat{x}, \hat{y}, \hat{z}$	Measured Translational Variables of Quadrotor
w_x, w_y, w_z	Translational Disturbance
a_x, a_y, a_z	Translational Acceleration of Quadrotor
x_{mt}, y_{mt}, z_{mt}	Actual Translational Variables of Moving Target
$\hat{x}_{mt}, \hat{y}_{mt}, \hat{z}_{mt}$	Measured Translational Variables of Moving Target
$a_x^{mt}, a_y^{mt}, a_z^{mt}$	Translational Acceleration of Moving Target
e_x, e_y, e_z	Target Tracking Errors
η	Rotational state vector
T_η	Sampling Time of Control Loop
ξ	Translational state vector
T_ξ	Sampling Time of Guidance Loop
B_x, B_y, B_z	Body-fixed Coordinate
E_x, E_y, E_z	Earth-fixed Coordinate
$T_i, i = 1, \ldots, 4$	Thrust Forces
I_{xx}, I_{yy}, I_{zz}	Moment of Inertia of the Quadrotor
m	Quadrotor's Mass
l	Length of Quadrotor's Arm
g	Gravitational Acceleration
$v_i, i = 1, \ldots, 4$	Normalised Input Voltage of each Motor
L_{FOV}^o	Actual Length of Field of View
L_{FOV}	Length of Truncated Field of View

https://doi.org/10.1017/aer.2021.23 Published online by Cambridge University Press

L_C	Length of Critical Region
L_{TR}	Length of Trusted Region
z_r	Altitude's Reference of Quadrotor
$\delta_x^{uav}, \delta_y^{uav}, \delta_z^{uav}$	Measuring Fault of Quadrotor's Position
$\delta_x^{mt}, \delta_y^{mt}, \delta_z^{mt}$	Measuring Fault of Target's Position
$\Delta_x, \Delta_y, \Delta_z$	Maximum Measuring Fault of Position
ϵ	Constant Adjustable Parameter
P_μ	Prediction Horizon
N_μ	Control Horizon
J_μ	Cost Function
E_{a_μ}	Input Vector of Cost Function
Y_{e_μ}	Output Vector of Cost Function
R_μ	Penalty Factor of Inputs
Q_μ	Penalty Factor of Outputs

1.0 INTRODUCTION

Tracking of ground moving targets (GMT) by unmanned aerial vehicles (UAVs) has a lot of military and commercial applications in aerial surveillance, traffic monitoring, border patrols, unmanned aerial/ground vehicles formation control, etc. The guidance and control of the UAVs to track a GMT has been investigated in several studies[1-3]. The complications of the target tracking are due to deceptive manoeuvering of targets, limitations of real-time data processing, target localisation error, terrain altitude variation, and departure of the target from the FOV.

Gomes et al.[1] proposed a UAV stabilisation strategy based on computer vision and switching controllers for GMT tracking. A visual servo controller is designed to keep multiple targets in the FOV of a mobile camera by Gans et al.[2]. Zhu et al.[3] proposed a saturated heading rate controller based on a guidance vector field to guarantee the global convergence of the UAV to a desired circular trajectory around the target. The geo-pointing control system is presented by Kim et al.[4]. This paper has discussed three main topics including estimating coordinates, tracking the stationary target, and flying automatically around the target. In another research, a vision system on a quadrotor is used to observe and track a visual target over a ground vehicle[5]. In the leader-follower formation control strategy, a combination of sliding mode control (SMC) and linear quadratic regulator (LQR) as the UAV local controller, and a pure-pursuit strategy as the unmanned ground vehicle (UGV) guidance law are used during takeoff, tracking and landing phases[6]. Engelhardt et al.[7] employed a flatness-based approach to obtain linear input-output dynamics as well as feasible reference trajectories using a MPC in which the operator commands are translated to the camera motions. Tan et al.[8] developed control and guidance laws for a quadrotor to track manoeuverable ground targets. In this reference, an optimal switching strategy is proposed, which is based on the analytic solutions of the proportional navigation and proportional derivative methods. Prevost et al.[9] proposed a two-level hierarchical approach for GMT tracking by a fixed wing UAV using MPC theory. Chen et al.[10] formulated the GMT tracking in cluttered environments using a quadrotor as an optimisation problem. In this approach, collision avoidance and dynamical feasibility are modeled as linear inequality constraints, which are considered in trajectory generation by the quadratic programming method. Kim et al.[11] proposed a nonlinear MPC

https://doi.org/10.1017/aer.2021.23 Published online by Cambridge University Press

framework for coordinated target tracking by a pair of unmanned aerial vehicles. The proposed controller is decentralised in which each UAV optimises its trajectory based on the prediction of the vehicles and target states. Oh et al.[12] proposed a guidance law for standoff target tracking based on the differential geometry between the UAV and the target to provide rigorous stability, explicit use of the target velocity, and tuning parameter reduction. Liu et al.[13] proposed an on-board vision-based system for tracking arbitrary 3D objects moving at unknown velocities by utilising a 3-axis gimbaled system. Moreover, a Kernelised Correlation Filter (KCF) tracker is used in that paper to detect and localise the target of interest from images acquired by the gimbaled camera, and proportional navigation (PN) guidance law is proposed as the tracking strategy. Yang et al.[14] addressed the problem of real-time object tracking for unmanned aerial vehicles via transforming the large-scale least-squares problem in the spatial domain to a series of small-scale least-squares problems with constraints in the Fourier domain using the correlation filter technique. Dong et al.[15] proposed a flight controller for a UAV to loiter over a GMT by designing a discrete-time integral sliding mode controller using an integral sliding surface. Liang et al.[16] studied the UAV/UGV collaborative tracking task as a heterogeneous system. In this paper, the deviation between the center of the ground vehicle and the center of the aerial image is used by the UAV as an error signal in a simple PID target tracker. Esposito et al.[17] proposed a vision-based system to autonomously detect and track an evader UAV with a moving camera. The proposed framework is based on a detection stage that exploits a Faster Region-based Convolution Neural Network to detect the region of interest associated with the UAVs position in the image plane.

Among the published research, few works have considered the models uncertainties in designing the guidance and control system[18-22]. Also, most of the strategies presented in the relevant literature haven't paid enough attention to the important requirements of the GMT tracking, such as terrain altitude variation, practical considerations include the UAV's dynamic constraints and the saturation of the actuators, the uncertainty of the target localisation, real-time implementation requirements, and the target temporal exit from the UAVs FOV.

Due to the uncertainty of the target localisation, the relative dynamics between the quadrotor and the target, and the multivariate nature of the problem, the MPC methodology is used to maintain the target at the center of the aerial images and reference altitude. Also, an altitude guidance law is employed to adjust the quadrotor FOV to the union of the desired trusted and critical regions. The dimensions of the desired trusted region are selected to be proportional to the non-compensated distance of the target from the center of the FOV. The critical region is a predefined margin around the trusted region, which is defined by an operator based on the upper bounds of the measurement errors of the quadrotor and the target positions. Also, it depends on the duration and the amount of increase in the target speed relative to the quadrotor speed. This three-dimensional guidance and control algorithm also can overcome changes in ground elevation, which causes the temporal exit of the target from the FOV.

The main contribution of this paper can be summarised as developing a three-dimensional guidance and control algorithm using the capability of adjusting the altitude of the quadrotor for preserving the manoeuverable target in the FOV, in the presence of wind, target localisation errors, and terrain altitude variation. The proposed approach finds the minimum altitude which preserves the target in the FOV in all circumstances. In other words, the proposed approach finds a balance between increasing the altitude, which is relevant for preserving the target in the FOV, and decreasing the altitude, which decreases the payload requirements.

The rest of the paper is organised as follows. The quadrotor nonlinear dynamics is represented briefly in Section 2. The proposed problem formulation and overall solution are

https://doi.org/10.1017/aer.2021.23 Published online by Cambridge University Press

discussed in Section 3. Section 4 is dedicated to the proposed MPC-based guidance and control law. A comprehensive simulation is performed in Section 5. Finally, conclusion and future works are presented.

2.0 QUADROTOR NONLINEAR DYNAMICS

It is assumed that the quadrotor has a rigid body and symmetrical structure. Also, the propellers of the motors are considered rigid which means that the flapping effects of propellers are negligible. Furthermore, the origin of the body-fixed frame coincides with the center of the gravity of the quadrotor and the thrust forces are proportional to the input voltage of the actuators. Two coordinate systems have been utilised including the body-fixed frame $B = [B_1, B_2, B_3]$ and the Earth-fixed frame as illustrated in Fig. 1. The dynamic model of the quadrotor, which is used in the current paper, is presented in detail in Ref. (23). This dynamic model is explained briefly in the following.

By employing the Euler-Lagrange equation, the nonlinear dynamic model is derived in the general form of $\dot{X} = F(X, U) + W$, in which $X \in R^{12}$, $U \in R^4$ and $W \in R^{12}$ are states, inputs, and aerodynamic disturbances, respectively[24]. The state vector consists of the quadrotor mass center position and the corresponding linear velocities of the quadrotor, i.e. $\xi = [z, \dot{z}, x, \dot{x}, y, \dot{y}]$, which is expressed in the Earth-fixed frame and the system attitude state vector, which is shown as $\eta = [\phi, \dot{\phi}, \theta, \dot{\theta}, \psi, \dot{\psi}]$.

According to the nature of the quadrotor dynamic model, it is usual to consider two separate subsystems, named rotational and translational subsystems containing ξ and η variables as it is mentioned by Bouabdallah et al.[25]. It should be noted that this consideration remains admissible for the relatively slow translational velocities.

Based on these descriptions, the state space representation of the rotational subsystem dynamic model is as follows[24].

$$\begin{bmatrix} \dot{\eta}_1 \\ \dot{\eta}_2 \\ \dot{\eta}_3 \\ \dot{\eta}_4 \\ \dot{\eta}_5 \\ \dot{\eta}_6 \\ v \end{bmatrix} = \begin{bmatrix} \eta_2 \\ a_1\eta_6\eta_4 + b_1(T_3 - T_1) \\ \eta_4 \\ a_2\eta_6\eta_2 + b_2(T_4 - T_2) \\ \eta_6 \\ a_3\eta_4\eta_2 + b_3(T_4 + T_2 - T_3 - T_1) \end{bmatrix} + \begin{bmatrix} 0 \\ w_\phi \\ 0 \\ w_\theta \\ 0 \\ w_\psi \end{bmatrix} \quad \ldots (1)$$

Also, the state space representation of the translational subsystem dynamic model is shown in Equation(2).

$$\begin{bmatrix} \dot{\xi}_1 \\ \dot{\xi}_2 \\ \dot{\xi}_3 \\ \dot{\xi}_4 \\ \dot{\xi}_5 \\ \dot{\xi}_6 \end{bmatrix} = \begin{bmatrix} \xi_2 \\ -g + \cos\eta_1 \cos\eta_3 \sum_{i=1}^{4} T_i/m \\ \xi_4 \\ (\cos\phi \sin\theta \cos\psi + \sin\phi \sin\psi) \sum_{i=1}^{4} T_i/m \\ \xi_6 \\ (\cos\phi \sin\theta \sin\psi - \sin\phi \cos\psi) \sum_{i=1}^{4} T_i/m \end{bmatrix} + \begin{bmatrix} 0 \\ w_z \\ 0 \\ w_x \\ 0 \\ w_y \end{bmatrix} \quad \ldots (2)$$

https://doi.org/10.1017/aer.2021.23 Published online by Cambridge University Press

Table 1
Quadrotor model parameters[24]

Parameters	Description
I_{xx}	Moment of inertia of the quadrotor around the E_x axis
I_{yy}	Moment of inertia of the quadrotor around the E_y axis
I_{zz}	Moment of inertia of the quadrotor around the E_y axis
m	Quadrotor mass
l_a	Quadrotor arm length
b	Thrust coefficient
g	Gravitational acceleration

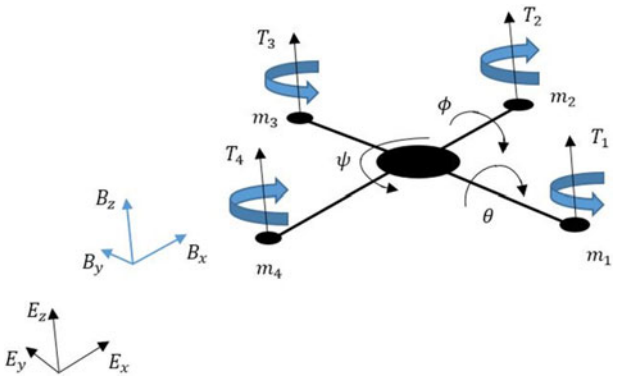

Figure 1. Body and earth coordinate systems used for quadrotor dynamic modeling.

The parameters used in the above equations are described in Table 1. Other parameters used for simplification in equations presentation are defined as follows.

$$a_1 = (I_{yy} - I_{zz})/I_{xx}, a_2 = (I_{zz} - I_{xx})/I_{yy}$$
$$a_3 = (I_{xx} - I_{yy})/I_{zz}, b_1 = l_a/I_{xx}, b_2 = l_a/I_{yy}$$
$$b_3 = 1/I_{zz}.$$

To apply the practical consideration, thrust forces are modeled as the following form.

$$T_i = k_1 v_i; \quad \text{with } 0 \le v_i \le 1 \text{ and } i = 1, 2, 3, 4 \qquad \ldots (3)$$

Also, the duty cycle of the actuators are considered using (4).

$$D_i = (h_0 v_i + h_1)/T_{pwm}; \quad \text{for } i = 1, 2, 3, 4 \qquad \ldots (4)$$

In Equation (3), v_i is normalised input voltage that corresponds to ith motor, which is typically in the range of zero to one, T_{pwm} is the duty cycle period, h_0 and h_1 are parameters relate to

https://doi.org/10.1017/aer.2021.23 Published online by Cambridge University Press

the dead zone and the saturation limit of the actuators, and k_1 is motor parameter obtained by a simple linear identification.

Substituting Equation (3) in Equations (2) and (1) yields the dynamic model of the system in the following form.

$$\begin{bmatrix}\dot{\eta}_1\\ \dot{\eta}_2\\ \dot{\eta}_3\\ \dot{\eta}_4\\ \dot{\eta}_5\\ \dot{\eta}_6\end{bmatrix} = \begin{bmatrix}\eta_2\\ a_1\eta_6\eta_4 + b_1k_1u_\phi\\ \eta_4\\ a_2\eta_6\eta_2 + b_2k_2u_\theta\\ \eta_6\\ a_3\eta_4\eta_2 + b_3k_3u_\psi\end{bmatrix} + \begin{bmatrix}0\\ w_\phi\\ 0\\ w_\theta\\ 0\\ w_\psi\end{bmatrix} \quad \ldots(5)$$

$$\begin{bmatrix}\dot{\xi}_1\\ \dot{\xi}_2\\ \dot{\xi}_3\\ \dot{\xi}_4\\ \dot{\xi}_5\\ \dot{\xi}_6\end{bmatrix} = \begin{bmatrix}\xi_2\\ -g + k_1\cos\eta_1\cos\eta_3u_z/m\\ \xi_4\\ k_1u_xu_z/m\\ \xi_6\\ k_1u_yu_z/m\end{bmatrix} + \begin{bmatrix}0\\ w_z\\ 0\\ w_x\\ 0\\ w_y\end{bmatrix} \quad \ldots(6)$$

in which

$$\begin{aligned} u_x &= \cos\phi\sin\theta\cos\psi + \sin\phi\sin\psi\\ u_y &= \cos\phi\sin\theta\sin\psi - \sin\phi\cos\psi\\ u_z &= \textstyle\sum_{i=1}^{4} v_i/m \end{aligned} \quad \ldots(7)$$

u_x and u_y are considered as virtual inputs while u_z and u_ϕ, u_θ, u_ψ are real inputs that correspond to the total thrust and the attitude of the quadrotor. The real inputs of the system are defined by the following equations.

$$\begin{bmatrix}v_1\\ v_2\\ v_3\\ v_4\end{bmatrix} = T^{-1}\begin{bmatrix}u_\phi\\ u_\theta\\ u_\psi\\ u_z\end{bmatrix}; \quad T = \begin{bmatrix}-1 & 0 & 1 & 0\\ 0 & -1 & 0 & 1\\ -1 & 1 & -1 & 1\\ 1 & 1 & 1 & 1\end{bmatrix}$$

It should be mentioned that the orientations of the quadrotor are restricted as follows.

$$\begin{bmatrix}-\pi/4\\ -\pi/4\\ -\pi\end{bmatrix} < \begin{bmatrix}\phi\\ \theta\\ \psi\end{bmatrix} < \begin{bmatrix}\pi/4\\ \pi/4\\ \pi\end{bmatrix}$$

https://doi.org/10.1017/aer.2021.23 Published online by Cambridge University Press

The dynamic model of the ground moving target is considered as follows, which corresponds to the accelerated three-dimensional motion of the target on the ground

$$\begin{bmatrix} \dot{\xi}_1^{mt} \\ \dot{\xi}_2^{mt} \\ \dot{\xi}_3^{mt} \\ \dot{\xi}_4^{mt} \\ \dot{\xi}_5^{mt} \\ \dot{\xi}_6^{mt} \end{bmatrix} = \begin{bmatrix} \xi_2^{mt} \\ 0 \\ \xi_4^{mt} \\ 0 \\ \xi_6^{mt} \\ 0 \end{bmatrix} + \begin{bmatrix} 0 \\ a_z^{mt} \\ 0 \\ a_x^{mt} \\ 0 \\ a_y^{mt} \end{bmatrix} \quad \ldots (8)$$

in which, $\xi^{mt} = [z_{mt}, \dot{z}_{mt}, x_{mt}, \dot{x}_{mt}, y_{mt}, \dot{y}_{mt}]$.

3.0 PROBLEM FORMULATION

As mentioned earlier, the possible altitude variation of the quadrotor can be used to prevent GMT loss.This section presents a guidance law and a sufficient condition to adjust the minimum quadrotor altitude for preserving the target in the FOV in long-term tracking. For this purpose, the FOV of the quadrotor is divided into two critical and trusted regions. The dimensions of the trusted region depend on the controller performance that is evaluated by the distance of the quadrotor from the target. The critical region is a predefined margin defined by an operator to prevent target loss in situations in which the target speed is temporally faster than the quadrotor speed. Also, it depends on the upper bounds of the quadrotor navigation errors and the target localisation errors. The proposed guidance law generates the minimum desired altitude of the quadrotor to adjust the FOV of the quadrotor to the union of the trusted and the critical regions.

Let P and $\hat{P}$ be considered as the real and the estimated position vector, respectively. *mt* and *uav* subscriptions are used through the paper to indicate the moving target and the unmanned aerial vehicle.

$$P_{uav} = \begin{bmatrix} x & y & z \end{bmatrix}, P_{mt} = \begin{bmatrix} x_{mt} & y_{mt} & z_{mt} \end{bmatrix},$$

$$\hat{P}_{uav} = \begin{bmatrix} \hat{x} & \hat{y} & \hat{z} \end{bmatrix}, \hat{P}_{mt} = \begin{bmatrix} \hat{x}_{mt} & \hat{y}_{mt} & \hat{z}_{mt} \end{bmatrix}$$

Definition 1. By considering z_r as the desired altitude reference; e_z, e_x and e_y, i.e. the estimated tracking errors, are defined by the following equations.

$$\begin{aligned} e_z &= \hat{z} - z_r \\ e_x &= \hat{x} - \hat{x}_{mt} \\ e_y &= \hat{y} - \hat{y}_{mt}. \end{aligned} \quad \ldots (9)$$

The uncertainty of the position measurements, which are denoted by δ_i^{uav} and δ_i^{mt} for the quadrotor and moving target positions, respectively, are shown in Equation (10). Without loss of generality, the upper bounds of these uncertainties are considered constant.

https://doi.org/10.1017/aer.2021.23 Published online by Cambridge University Press

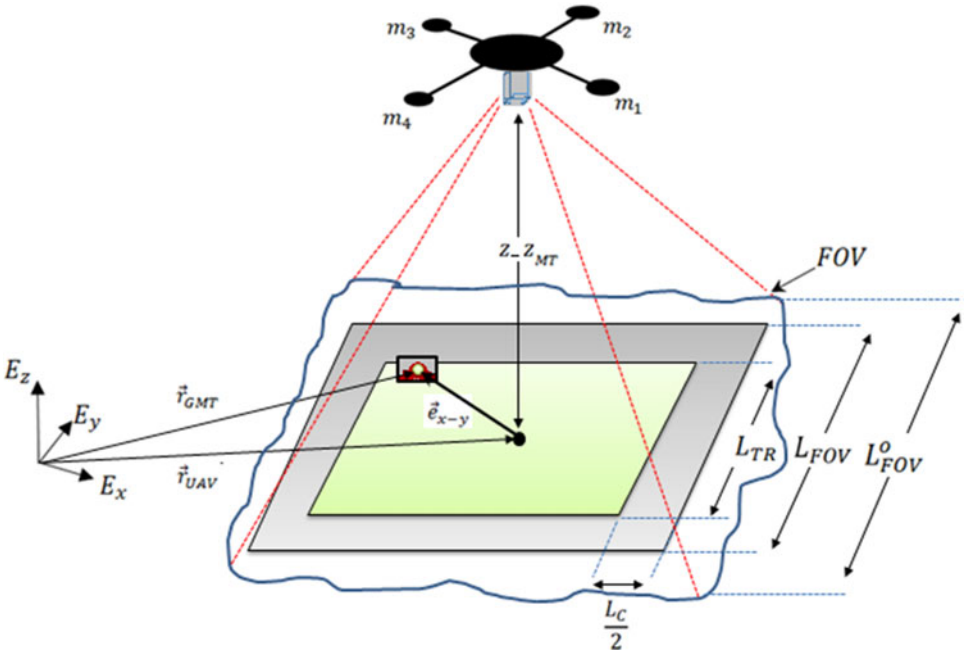

Figure 2. Illustration of the parameters used in the problem formulation.

$$\begin{aligned}
\hat{x}_{mt} &= x_{mt} \pm \delta_x^{mt} \\
\hat{y}_{mt} &= y_{mt} \pm \delta_y^{mt} \\
\hat{z}_{mt} &= z_{mt} \pm \delta_z^{mt} \\
\hat{x} &= x \pm \delta_x^{uav} \\
\hat{y} &= y \pm \delta_y^{uav} \\
\hat{z} &= z \pm \delta_z^{uav}.
\end{aligned} \quad \ldots(10)$$

As illustrated in Fig. 2, e_{x-y} is the target tracking error in the horizontal plan and L^o_{FOV} is the actual size of the smaller dimension of the field of view (FOV). To simplify the derivation and improvement of the proposed approach, a square FOV with L_{FOV} dimensions is defined as a subset of the actual FOV which results the following relation;

$$L_{FOV} \leq L^o_{FOV} \quad \ldots(11)$$

The considered square FOV is divided into critical and trusted regions. The dimensions of these regions are shown with L_C and L_{TR}. Based on this description, it can be written;

$$L_{FOV}(\hat{z}) = L_{TR}(\hat{z}) + L_C \quad \ldots(12)$$

As denoted in Equation (12), the dimensions of the critical region remain constant through an operation, which are set by the operator. However, L_{FOV} and L_{TR} are functions of the altitude of the quadrotor. In fact, L_{FOV} will be equal to the L_C when the tracking error (e_{x-y} in Fig. 2) becomes zero (13).

https://doi.org/10.1017/aer.2021.23 Published online by Cambridge University Press

$$L_{FOV}(z_0) = L_C. \quad \ldots(13)$$

In Equation (13), z_0 is the required altitude of the quadrotor to provide a FOV with L_C dimension.

The following assumptions are considered to develop the proposed strategy:

Assumption 1. Without loss of generality and to simplify the equations, the direction of the camera is considered vertical to the $x-y$ plane, which can be provided by a simple local controller for the employed two axis gimbaled camera. Generally, the controller should maintain the direction of the camera on fixed values or measure them. In this manner, the captured aerial image should be compensated by the camera angles. The other phases of the proposed approach are the same as following.

Assumption 2. Both angles of field of view of the camera are assumed to be larger than 45 degrees, which means $L^o_{FOV}(k) \geq \hat{z}(k) - \hat{z}_{mt}(k)$ for $k \geq 0$.

3.1 Critical region design

L_C is a constant value composed of ϵ and Δ_{x-y-z} as follows.

$$L_C = \epsilon + \Delta_{x-y-z}; \quad \epsilon > 0, \quad \Delta_{x-y-z} > 0 \quad \ldots(14)$$

In the Equation (14), ϵ is used to prevent the target loss when the target speed is temporarily faster than the quadrotor speed. Its value is designed by the operator based on the maximum estimated duration and the amount of difference between the quadrotor and the target speed. Also, Δ_{x-y-z} is an upper bound for the effect of measurement errors on the horizontal plane, which is defined by the following equation

$$\Delta_{x-y-z} = 2 * (\Delta_z + \Delta_{x-y}), \quad \ldots(15)$$

where Δ_z is an equivalent value for the quadrotor and target al.titude measurement errors ($\bar{\Delta}_z$) on the horizontal plane containing the target.

$$\Delta_{x-y} = \max(|\bar{\delta}^{uav}_x| + |\bar{\delta}^{mt}_x|, |\bar{\delta}^{uav}_y| + |\bar{\delta}^{mt}_y|).$$
$$\bar{\Delta}_z = |\bar{\delta}^{mt}_z| + |\bar{\delta}^{uav}_z|$$

As previously mentioned about Equation (10), $\bar{\delta}^{uav}_i$ and $\bar{\delta}^{mt}_i$ are the upper bounds of the quadrotor and the moving target localisation errors, respectively. i in this parameters denote the x,y,z directions.

It should be mentioned that the average speed of the quadrotor should be bigger than the average speed of the target in a long-term tracking scenario. The proposed algorithm is designed to be robust to the temporary increase in the target velocity in relation to the quadrotor velocity.

3.2 Trusted region design

L_{TR} is an ascending function of the quadrotor altitude that means increasing in the quadrotor altitude causes the larger dimentions of L_{TR}. Considering the relation between $L_{FOV}(z)$, and the

https://doi.org/10.1017/aer.2021.23 Published online by Cambridge University Press

critical and the trusted regions dimensions mentioned in Equation (12) and the Assumption 2, a suitable function between L_{TR} and the quadrotor altitude that satisfies the marginal constraint in Equation (13) can be as follows.

$$L_{TR}(\hat{z}) = \begin{cases} \hat{z}(k) - z_0(k) & \hat{z}(k) > z_0(k) \\ 0 & Else \end{cases} \quad \ldots(16)$$

A sufficient condition to preserve the target in the FOV will be proven through the three following lemmas. In the thired one, the desired altitude of the quadrotor is determined based on the designed trusted region. Also, a sufficient condition for the loss of target during the ususal target tracking without the FOV adjustment will be proven in the last lemma.

Lemma 1. *To satisfy the inequality (11), it is enough to determine z_0 as*

$$z_0 \geq L_C + \hat{z}_{mt}.$$

Proof. Substituting Equation (16) in Equation (12) takes the following form.

$$L_{FOV}(\hat{z}) = \hat{z}(k) - z_0 + L_C = \hat{z}(k) - \hat{z}_{mt} - (z_0 - \hat{z}_{mt} - L_C) \quad \ldots(17)$$

Considering the Assumption 2 and the z_0 determination, which means $z_0 - \hat{z}_{mt} - L_C$ is not negative, (17) can be rewritten as the following inequality.

$$L_{FOV}(\hat{z}) \leq \hat{z}(k) - \hat{z}_{mt} \leq L^o_{FOV}(k).$$

Lemma 2. *The real and the estimated distances between the quadrotor and the target satisfy the following inequalities.*

$$\begin{aligned} |x - x_{mt}| &< |e_x| + \Delta_{x-y} \\ |y - y_{mt}| &< |e_y| + \Delta_{x-y} \\ |x - x_{mt}| &> |e_x| - \Delta_{x-y} \\ |y - y_{mt}| &> |e_y| - \Delta_{x-y} \end{aligned}$$

Proof. Substituting Equation (10) in Equation (9), the following equations are obtained.

$$\begin{aligned} e_x &= x - x_{mt} \pm \delta_x^{uav} \pm \delta_x^{mt} \\ e_y &= y - y_{mt} \pm \delta_y^{uav} \pm \delta_y^{mt}, \end{aligned} \quad \ldots(18)$$

Considering the definition of Δ_{x-y} in the critical region design, it is straightforward to derive the Lemma 2 from Equation (18).

Lemma 3. *A sufficient condition to maintain the target in the FOV is defined as follows.*

$$e_z(k) + \epsilon > 0 \quad ; e_z = \hat{z} - z_r \quad \ldots(19)$$

https://doi.org/10.1017/aer.2021.23 Published online by Cambridge University Press

which is provided by

$$z_r(k) = 2\max(|e_x|, |e_y|) + z_0(k) \quad \ldots(20)$$

Proof. To preserve the target in the field of view of the quadrotor, the following inequality should be satisfied.

$$L_{FOV}/2 > \max(|x - x_{mt}|, |y - y_{mt}|), \quad for\ k > 0 \quad \ldots(21)$$

Applying the Lemma 2 to the inequality (21) results the following inequality.

$$L_{FOV}/2 > \max(|e_x| + \Delta_{x-y}, |e_y| + \Delta_{x-y}) \quad \ldots(22)$$

Substituting Equations (15) and (12) in Equation (22) yields the following relation.

$$L_{TR}(\hat{z})/2 + \epsilon/2 > \max(|e_x|, |e_y|) \quad \ldots(23)$$

Defining $e_{L_{TR}} = L_{TR}(\hat{z}) - L_{TR}(z_r)$, Equation (23) takes the following form.

$$e_{L_{TR}}/2 + \epsilon/2 > \max(|e_x|, |e_y|) - L_{TR}(z_r)/2 \quad \ldots(24)$$

To eliminate the right side of the inequality (24), $L_{TR}(z_r)$ is designed using the following form.

$$L_{TR}(z_r) = 2\max(|e_x|, |e_y|). \quad \ldots(25)$$

According to Equations (16) and (25), the desired altitude of the quadrotor to preserve the target in the FOV is determined as follows.

$$z_r(k) = 2\max(|e_x|, |e_y|) + z_0(k) \quad \ldots(26)$$

Using Equations (16) and (26), $e_{L_{TR}}$ changes to the following form.

$$e_{L_{TR}} = \hat{z}(k) - z_0(k) - z_r(k) + z_0(k) = e_z(k) \quad \ldots(27)$$

Substituting Equations (25) and (27) in Equation (24), the Lemma 3 inequality is obtained.

Lemma 4. *Considering the assumption $L^o_{FOV} = L_{FOV}$, a sufficient condition for the loss of the target using the usual target tracking approach without the FOV adjustment by the altitude increasing is defined as follows.*

$$e_z(k) + \epsilon - 2\min(|e_x|, |e_y|) < 0; \quad e_z = \hat{z} - z_r \quad \ldots(28)$$

which is provided by

$$z_r(k) = z_0(k) \quad \ldots(29)$$

https://doi.org/10.1017/aer.2021.23 Published online by Cambridge University Press

Proof. To lose the target from the field of view of the quadrotor, the following inequality should be satisfied.

$$L_{FOV}/2 < \min(|x - x_{mt}|, |y - y_{mt}|), \quad for\ k > 0 \qquad \ldots(30)$$

Applying the Lemma 2 to the inequality (30), the following inequality is obtained.

$$L_{FOV}/2 < \min(|e_x| - \Delta_{x-y}, |e_y| - \Delta_{x-y}) \qquad \ldots(31)$$

Substituting Equations (15) and (12) in Equation (31) yields the following relation.

$$L_{TR}(\hat{z})/2 + \epsilon/2 < \min(|e_x|, |e_y|); \quad \epsilon \pm \Delta_z \approx \epsilon \qquad \ldots(32)$$

Defining $e_{L_{TR}} = L_{TR}(\hat{z}) - L_{TR}(z_r)$, Equation (32) takes the following form.

$$e_{L_{TR}}/2 + \epsilon/2 < \min(|e_x|, |e_y|) - L_{TR}(z_r)/2 \qquad \ldots(33)$$

In the usuall approaches without the proposed strategy in the inequality (33), $L_{TR}(z_r)$ is selected as follows.

$$L_{TR}(z_r) = 0 \qquad \ldots(34)$$

According to Equations (16) and (34), the reference altitude of the quadrotor is determined as the follows.

$$z_r(k) = z_0(k) \qquad \ldots(35)$$

Using Equations (16) and (35), $e_{L_{TR}}$ changes to the following form.

$$e_{L_{TR}} = \hat{z}(k) - z_0(k) - z_r(k) + z_0(k) = e_z(k) \qquad \ldots(36)$$

Substituting Equations (34) and (36) to Equation (33), yields the inequality of Lemma 4. □

4.0 MPC-BASED GUIDANCE AND CONTROL

As shown in the previous section, to maintain the target in the FOV of the quadrotor, it is sufficient to satisfy the inequality of (19) when designing the guidance law. Given this fact, and without loss of generality, a feedback linearision (FL) is applied to the nonlinear model to achieve a decoupled linear description of the system. Furthermore, the position error vector integral is added to the model to achieve null steady errors in the presence of wind disturbances[19]. The proposed MPC-based guidance and control system consist of three main components, the quadrotor desired attitude generator, the reference $x - y$ planar motion generator, and the desired attitude generator in a cascade structure. It should be noted that such cascade architecture requires slower translational dynamics than rotational ones. The guidance and control diagram including the non-linear system dynamic and the actuator model is illustrated in Fig. 3.

https://doi.org/10.1017/aer.2021.23 Published online by Cambridge University Press

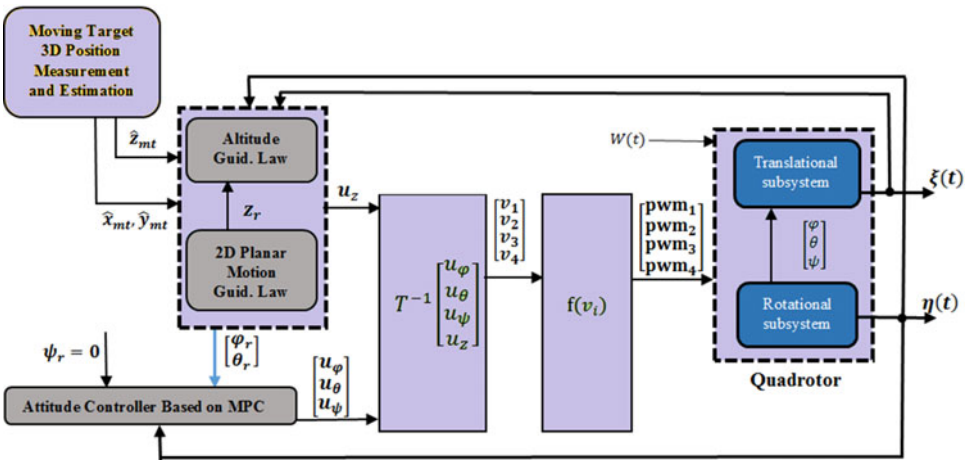

Figure 3. Block diagram of the MPC-based guidance and control subsystem.

4.1 Linear decoupled dynamic of the quadrotor

Initially, a linear decoupled dynamics of the quadrotor must be derived. To meet this need, primitive nonlinear feedbacks for rotational and translational subsystems are considered in the following forms, respectively.

$$\begin{aligned} u_\phi &= -(a_1\eta_4\eta_6 - a_\phi)/c_1 \\ u_\theta &= -(a_3\eta_2\eta_6 - a_\theta)/c_2 \\ u_\psi &= -(a_5\eta_2\eta_4 - a_\psi)/c_3 \end{aligned} \quad \ldots(37)$$

$$\begin{aligned} u_z &= m(g + a_z)/(k_1 \cos\eta_1 \cos\eta_3) \\ u_x &= ma_x/k_1u_z \\ u_y &= ma_y/k_1u_z \end{aligned} \quad \ldots(38)$$

where, $V = [a_\phi, a_\theta, a_\psi, a_z, a_x, a_y]$ is the quadrotor movement acceleration vector.

Substituting Equation (37) in Equation (5) yields three decoupled identical linear dynamics for the rotational subsystem as shown in Equation (39).

$$\begin{aligned} \dot{\eta}^s &= A_m\eta^s + B_m a_\eta^s \quad \text{for } s = 0, 1, 2 \\ y_\eta^s &= C_m\eta^s \end{aligned} \quad \ldots(39)$$

where

$\eta^0 = [\phi, \dot{\phi}]^T, \eta^1 = [\theta, \dot{\theta}]^T, \eta^2 = [\psi, \dot{\psi}]^T$

$$A_m = \begin{bmatrix} 0 & 1 \\ 0 & 0 \end{bmatrix} \quad B_m = \begin{bmatrix} 0 \\ 1 \end{bmatrix} \quad C_m = \begin{bmatrix} 1 & 0 \end{bmatrix}$$

$a_\eta^0 = a_\phi \; a_\eta^1 = a_\theta \; a_\eta^2 = a_\psi$

Also, substituting the Equation (38) into the Equation (6) yields three decoupled identical linear dynamics for the translational subsystem as follows.

https://doi.org/10.1017/aer.2021.23 Published online by Cambridge University Press

$$\begin{aligned}\dot{\xi}^s &= A_m\xi^s + B_m a_\xi^s + B_m w_\xi^s \quad \text{for } s = 0, 1, 2\\ y_\xi^s &= C_m\xi^s\end{aligned} \qquad \ldots(40)$$

in which

$\xi^0 = [z, \dot{z}]^T, \xi^1 = [x, \dot{x}]^T, \xi^2 = [y, \dot{y}]^T$

$$\begin{bmatrix} a_\xi^0 \\ w_\xi^0 \end{bmatrix} = \begin{bmatrix} a_z \\ w_z \end{bmatrix}, \begin{bmatrix} a_\xi^1 \\ w_\xi^1 \end{bmatrix} = \begin{bmatrix} a_x \\ w_x \end{bmatrix}, \begin{bmatrix} a_\xi^2 \\ w_\xi^2 \end{bmatrix} = \begin{bmatrix} a_y \\ w_y \end{bmatrix}$$

GMT dynamics in the Equation (8) can be written as

$$\dot{\xi}_{mt}^s = A_m\xi_{mt}^s + B_m a_{mt}^s \quad \text{for } s = 0, 1, 2 \qquad \ldots(41)$$

in which

$\xi_{mt}^0 = [z_{mt}, \dot{z}_{mt}]^T, \xi^1 = [x_{mt}, \dot{x}_{mt}]^T, \xi^2 = [y_{mt}, \dot{y}_{mt}]^T$

$a_{mt}^0 = a_z^{mt}, a_{mt}^1 = a_x^{mt}, a_{mt}^2 = a_y^{mt}$

The virtual reference air vehicle defined in Ref. (19) has a linear dynamic model similar to the quadrotor rotational subsystem.

$$\dot{\eta}_r^s = A_m\eta_r^s + B_m a_{\eta_r}^s \quad \text{for } s = 0, 1, 2 \qquad \ldots(42)$$

where, $\eta_r^0 = [\phi_r, \dot{\phi}_r]^T$, $\eta_r^1 = [\theta_r, \dot{\theta}_r]^T$, and $\eta_r^2 = [\psi_r, \dot{\psi}_r]^T$. Based on Equation (39), the linear acceleration reference values, i.e. $a_{\eta_r}^s$ can be defined as follows.

$$a_{\eta_r}^0 = a_{\phi_r} = \ddot{\phi}_r, a_{\eta_r}^1 = a_{\theta_r} = \ddot{\theta}_r, a_{\eta_r}^2 = a_{\psi_r} = \ddot{\psi}_r$$

To achieve zero steady state position errors, the augmented translational error vector is defined as follows.

$$e_\xi^0 = \begin{bmatrix} e_z \\ \dot{e}_z \\ \int e_z \end{bmatrix} = \begin{bmatrix} \hat{z} - z_r \\ \dot{z} - \dot{z}_{mt} - \dot{L}_c^{des} \\ \int \hat{z} - z_r \end{bmatrix}$$

$$e_\xi^1 = \begin{bmatrix} e_x \\ \dot{e}_x \\ \int e_x \end{bmatrix} = \begin{bmatrix} \hat{x} - \hat{x}_{mt} \\ \dot{x} - \dot{x}_{mt} \\ \int \hat{x} - \hat{x}_{mt} \end{bmatrix} \qquad \ldots(43)$$

$$e_\xi^2 = \begin{bmatrix} e_y \\ \dot{e}_y \\ \int e_y \end{bmatrix} = \begin{bmatrix} \hat{y} - \hat{y}_{mt} \\ \dot{y} - \dot{y}_{mt} \\ \int \hat{y} - \hat{y}_{mt} \end{bmatrix},$$

Substituting the Equations (40) and (41) in the Equation (43), the dynamics of the translational error is written as follows.

https://doi.org/10.1017/aer.2021.23 Published online by Cambridge University Press

$$\begin{aligned}\dot{e}^s_\xi(t) &= Ae^s_\xi + Be^s_{a_\xi}(t) + Bw^s_\xi(t) \quad \text{for } s = 0, 1, 2\\ e^s_{y_\xi}(t) &= Ce^s_\xi(t),\end{aligned} \quad \ldots(44)$$

in which

$e^0_{a_\xi} = \ddot{z} - \ddot{z}_r = a_z - a^{mt}_z - 2\max(|e^1_{a_\xi}|, |e^2_{a_\xi}|)$, $e^1_{a_\xi} = \ddot{x} - \ddot{x}_{mt} = a_x - a^{mt}_x$, $e^2_{a_\xi} = \ddot{y} - \ddot{y}_{mt} = a_y - a^{mt}_y$

$$A = \begin{bmatrix}0 & 1 & 0\\ 0 & 0 & 0\\ 1 & 0 & 0\end{bmatrix}, B = \begin{bmatrix}0\\ 1\\ 0\end{bmatrix}, C = \begin{bmatrix}1 & 0 & 0\end{bmatrix}$$

By subtracting the Equation (39) from the Equation (42) and augmenting the attitude errors, the rotational error dynamics model is obtained as follows.

$$\begin{aligned}\dot{e}^s_\eta(t) &= Ae^s_\eta + Be^s_{a_\eta}(t) + Bw^s_\eta(t) \quad \text{for } s = 0, 1, 2\\ e^s_{y_\eta}(t) &= Ce^s_\eta(t),\end{aligned} \quad \ldots(45)$$

where, $e^s_\eta = \begin{bmatrix}\eta^s_1 - {\eta_1}^s_r\\ \eta^s_2 - {\eta_2}^s_r\\ \int(\eta^s_1 - {\eta_1}^s_r)\end{bmatrix}$, $e^s_{a_\eta} = a^s_\eta - a^s_{\eta r}$

Considering the measurement rate of the sensors, T_ξ and T_η are defined as the sampling period for the guidance and control loops, respectively.

The discrete representation of the quadrotor error dynamics takes the following form[19] for $s = 0, 1, 2$.

$$\begin{aligned}e^s_\xi(k+1) &= A_\xi e^s_\xi(k) + B_\xi e^s_{a_\xi}(k) + B_\xi w^s_\xi(k)\\ e^s_{y_\xi}(k) &= Ce^s_\xi(k),\end{aligned} \quad \ldots(46)$$

$$\begin{aligned}e^s_\eta(k+1) &= A_\eta e^s_\eta(k) + B_\eta e^s_{a_\eta}(k) + Bw^s_\eta(k)\\ e^s_{y_\eta}(k) &= Ce^s_\eta(k),\end{aligned} \quad \ldots(47)$$

in which

$$A_\xi = \begin{bmatrix}1 & T_\xi & 0\\ 0 & 1 & 0\\ T_\xi & 0 & 1\end{bmatrix}, B_\xi = \begin{bmatrix}0\\ T_\xi\\ 0\end{bmatrix},$$

$$A_\eta = \begin{bmatrix}1 & T_\eta & 0\\ 0 & 1 & 0\\ T_\eta & 0 & 1\end{bmatrix}, B_\eta = \begin{bmatrix}0\\ T_\eta\\ 0\end{bmatrix}$$

Using μ to indicate both η and ξ subscriptions, the error dynamics, mentioned in Equations (46) and (47), can be written in a common form as follows.

https://doi.org/10.1017/aer.2021.23 Published online by Cambridge University Press

$$\begin{aligned} e^s_\mu(k+1) &= A_\mu e^s_\mu(k) + B_\mu e^s_{a_\mu}(k) \\ e^s_{y_\mu}(k) &= C e^s_\mu(k). \end{aligned} \quad \text{for} \begin{cases} s = 0, 1, 2 \\ \mu = \xi, \eta \end{cases} \quad \ldots (48)$$

4.2 Guidance and control synthesis

In the previous subsection, the guidance and control problem for a nonlinear high order system is simplified to a linear third-order model. In this section, the MPC formulation is discussed for the Equation (48), which is common for $s = 0, 1, 2$. It should be noted that unknown effects on the system such as unmeasurable disturbance are excluded from Equation (48).

J_μ is considered as a cost function that has the following form[26].

$$J^s_\mu = {Y^s_{e_\mu}}^T Q^s_\mu Y^s_{e_\mu} + {E^s_{a_\mu}}^T R^s_\mu E^s_{a_\mu} \quad for \begin{cases} s = 0, 1, 2 \\ \mu = \xi, \eta \end{cases} \quad \ldots (49)$$

in which

$$Y^s_{e_\mu} = \begin{bmatrix} e^s_{y_\mu}(k+1|k) \\ e^s_{y_\mu}(k+2|k) \\ \vdots \\ e^s_{y_\mu}(k+P_\mu|k) \end{bmatrix} \quad E^s_{a_\mu} = \begin{bmatrix} \hat{e}^s_{a_\mu}(k) \\ \hat{e}^s_{a_\mu}(k+1) \\ \vdots \\ \hat{e}^s_{a_\mu}(k+N_\mu-1) \end{bmatrix},$$

and the P_μ, N_μ are the prediction and the control horizon parameters, respectively. Also, the $Q_\mu \geq 0, R_\mu > 0$ are penalty factors related to the errors and the inputs, respectively. α_μ is the pole of the first order filter on the reference signal to suppress its abrupt changes, as well as noise effects[27]. The guidance law is obtained by solving the optimisation problem in the following form.

$$\begin{aligned} {E^s_{a_\mu}}^* = \underset{E^s_{a_\mu}}{\text{minimize}} \quad & J^s_\mu \quad \text{for} \begin{cases} s = 0, 1, 2 \\ \mu = \xi, \eta \end{cases} \\ \text{subject to} \quad & Y^s_{e_\mu} = F_\mu e^s_\mu(k) + G_\mu e^s_{a_\mu}(k) \\ & \underline{Y}^s_{e_\mu} \leq Y^s_{e_\mu} \leq \overline{Y}^s_{e_\mu} \\ & \underline{E}^s_{a_\mu} \leq E^s_{a_\mu} \leq \overline{E}^s_{a_\mu} \end{aligned} \quad \ldots (50)$$

where

$$F_\mu = \begin{bmatrix} CA_\mu & CA^2_\mu & CA^3_\mu & \ldots & CA^P_\mu \end{bmatrix}^T$$

$$G_\mu = \begin{bmatrix} CB_\mu & 0 & \ldots & 0 \\ CA_\mu B_\mu & C_\mu B_\mu & \ldots & 0 \\ CA^2_\mu B_\mu & CA_\mu B_\mu & \ldots & 0 \\ \vdots & & & \\ CA^{P-1}_\mu B_\mu & CA^{P-2}_\mu B_\mu & \ldots & CA^{P-N}_\mu B_\mu \end{bmatrix}$$

https://doi.org/10.1017/aer.2021.23 Published online by Cambridge University Press

Initial conditions of the dynamic model at instance kth is provided by the measurement of the system at the same time.

Optimisation methods such as quadratic programming can be used to solve the problem (50). In this approach, an optimisation should be performed at any time. The closed form is obtained by replacing of $Y^s_{e_\mu}$ in the Equation (49) and derivation with respect to $e^s_{a_\mu}(k)$, as the following equation[27]:

$$E^{s}_{a_\mu}{}^{*} = -\left(G^T_\mu Q_\mu G_\mu + R_\mu\right)^{-1} G^T_\mu Q_\mu F_\mu e_\mu(k) \quad \ldots(51)$$

High computational burden and consumption time are prominent disadvantages of the optimisation methods. Given this, Equation (51) is employed as the solution of the optimisation problem (50) to derive the desired relative acceleration for the $x-y$ planar motion. This provides the admissible performance of the proposed algorithm. It should be noted that inequality constraints can be satisfied via adjusting Q_μ and R_μ parameters[27]; however, in the considered case, it is assumed that inequality constraints remain passive using powerful actuators.

To obtain the desired relative acceleration for altitude, the inequality constraint (19) should be satisfied. For this purpose, the following algorithm is proposed

- Initially, the solution of Equation (51) is used to obtain $\hat{e}^0_{a_\xi}(k)$
- If $e_z(k+1|k)+\epsilon > 0 \rightarrow A_\xi e^0_\xi(k) + B_\xi \hat{e}^0_{a_\xi}(k) + \epsilon > 0$ then $(\hat{e}^0_{a_\xi})^* = \hat{e}^0_{a_\xi}$
- Else, numerical optimisation algorithms such as QP is employed for solving Equation (50) subject to $-\epsilon \left[1\ 1\ \ldots\ 1\right] < Y^0_{e_\xi}$.

Subsequently, the appropriate translational acceleration, which reduces the distance between the quadrotor and the target, takes the following form.

$$\begin{aligned} a^{0\,des}_\xi &= a^{des}_z(k) = \hat{a}^{mt}_z + \left(\hat{e}^0_{a_\xi}\right)^* + 2\max\left(|e^1_{a_\xi}|, |e^2_{a_\xi}|\right) \\ a^{1\,des}_\xi &= a^{des}_x(k) = \hat{a}^{mt}_x + \left(\hat{e}^1_{a_\xi}\right)^* \\ a^{2\,des}_\xi &= a^{des}_y(k) = \hat{a}^{mt}_y + \left(\hat{e}^2_{a_\xi}\right)^*, \end{aligned} \quad \ldots(52)$$

where, $\hat{a}^{mt}_z$, $\hat{a}^{mt}_x$ and $\hat{a}^{mt}_y$ are the measured acceleration of the moving target described by the following equations.

$$\begin{aligned} \hat{a}^{mt}_z &= a^{mt}_z \pm \delta^{mt}_{a_z} \\ \hat{a}^{mt}_x &= a^{mt}_x \pm \delta^{mt}_{a_x} \\ \hat{a}^{mt}_y &= a^{mt}_y \pm \delta^{mt}_{a_y}, \end{aligned} \quad \ldots(53)$$

where $\delta^{mt}_{a_z}$, $\delta^{mt}_{a_z}$ and $\delta^{mt}_{a_z}$ are estimation errors.

After calculating the desired translational acceleration, $u_z(k)$ and the reference of the roll and pitch angles, i.e. ϕ_r and θ_r, are derived using Equations (7) and (38). These references should be provided for the quadrotor rotational loop as follows.

https://doi.org/10.1017/aer.2021.23 Published online by Cambridge University Press

Table 2
MPC-based guidance and control parameters

Parameters	Rotational controller	Translational controller
$P(s)$	1	3
$M(s)$	1	2
α	0.1	0.1
Q	$diag[1, 1, 2]$	$diag[500, 500, 1000]$
R	10	1
$f(h)$	100	10
$T_s(s)$	0.01	0.1

$$
\begin{aligned}
u_z(k) &= m\frac{a_z^{des}(k)+g}{k_1\cos(\phi_k)\sin(\theta_k)} \\
\phi_r(k) &= \arcsin\left(\frac{ma_x^{des}(k)}{k_1u_z(k)}\sin(\psi_k)-\frac{ma_y^{des}(k)}{k_1u_z(k)}\cos(\psi_k)\right) \\
\theta_r(k) &= \arcsin\left(\frac{a_x^{des}(k)\cos(\psi_k)+a_y^{des}(k)\sin(\psi_k)}{\sqrt{\left(\frac{k_1u_z(k)}{m}\right)^2-\left(a_x^{des}(k)\sin(\psi_k)-a_y^{des}(k)\cos(\psi_k)\right)^2}}\right)
\end{aligned}
\quad \ldots(54)
$$

Similarly, the desired rotational accelerations $a_\phi^{des}(k)$, $a_\theta^{des}(k)$ and $a_\psi^{des}(k)$ have been computed to track attitude reference signals by the quadrotor.

$$
a_\eta^{s\,des}(k) = a_{\eta_r}^s(k) + \left(\hat{e}_{a_\eta}^s(k)\right)^* \quad \text{for } s=0,1,2 \qquad \ldots(55)
$$

in which the $(\hat{e}_{a_\eta}^s(k))^*$ is the first component of ${E_{a_\mu}^s}^*$ in Equation (51).

General control inputs, i.e. $u_\phi(k), u_\theta(k)$ and $u_\psi(k)$, can be generated by substituting Equation (55) in Equation (37).

The corresponding duty cycles of the quadrotor actuators are obtained using the Equation (4) presented in Section 4.

5.0 SIMULATION RESULTS

The MPC parameters presented in Table 2 are designed to achieve fast disturbance rejection and smooth output tracking. The sample time is selected to provide sufficient opportunity for the translational controller to track the predefined trajectory using the roll and pitch angles produced by the rotational controller.

The initial condition is defined in such a way that satisfies Equation (19) at $k=0$, i.e. $e_z(0)+\epsilon>0$. The simulations are performed for the following initial condition of the translational and rotational subsystems, respectively.

https://doi.org/10.1017/aer.2021.23 Published online by Cambridge University Press

Table 3
Problem formulation parameters

Parameters	Value	Parameters	Value
$\bar{\delta}_x^{mt} = \bar{\delta}_z^{mt}$ (cm)	10	$\bar{\delta}_x^{uav} = \bar{\delta}_z^{uav}$ (cm)	10
$\bar{\delta}_y^{mt}$ (cm)	15	$\bar{\delta}_y^{uav}$ (cm)	15
Δ_{x-y} (cm)	30	Δ_z (cm)	20
ϵ (cm)	200	$\Delta z0$ (cm)	280

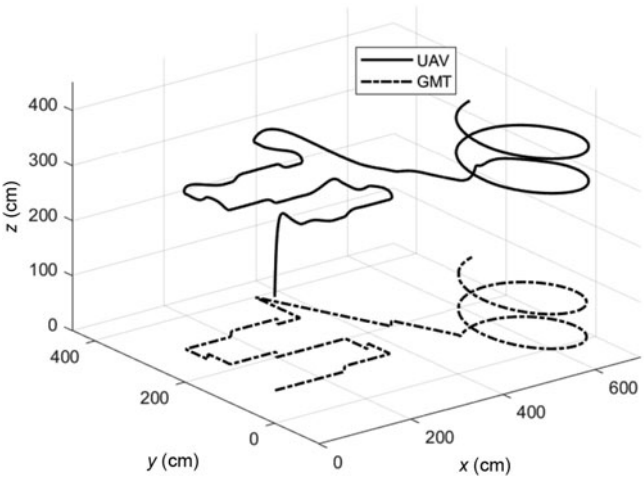

Figure 4. The 3D trajectories of the ground moving target and the tracker UAV.

$$\xi(0) = \begin{bmatrix} 200 & 0 & 50 & 0 & 50 & 0 \end{bmatrix}$$
$$\eta(0) = \begin{bmatrix} 0 & 0 & 0 & 0 & 0 & 0 \end{bmatrix}$$

Problem formulation parameters are listed in Table 3. The quadrotor parameters are selected based on a real model, which are as follows.

$$I_{xx} = I_{yy} = 0.0069\text{kg.m}^2 \quad I_{zz} = 0.0137\text{kg.m}^2$$
$$J_r = 0.0000551\text{kg.m}^2 \; l_a = 0.27\text{m}$$

Sinusoidal external disturbances on the six degrees of freedom are included. The magnitude of disturbances on the aerodynamic forces and moments have been set as in Ref. (24).

$$w_x = 2u(t-70)\cos t(\text{N/kg}) w_\phi = u(t-130)\sin t(\text{N.m})$$
$$w_y = 2u(t-100)\cos t(\text{N/kg}) w_\theta = u(t-170)\cos t(\text{N.m})$$
$$w_z = u(t-40)\sin t(\text{N/kg}) w_\psi = u(t-200)\cos t\,(\text{N.m})$$

Figures 4–11. show the tracking results in such a way that there is no error in estimating the target acceleration. This is not a general assumption and will be removed in the next

https://doi.org/10.1017/aer.2021.23 Published online by Cambridge University Press

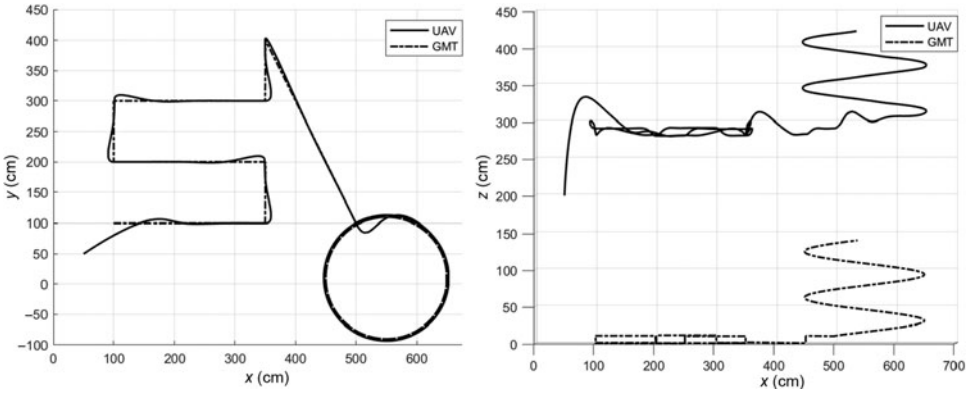

Figure 5. The 2D illustration of the ground moving target and the tracker UAV trajectories on the $x - y$ and $x - z$ planes.

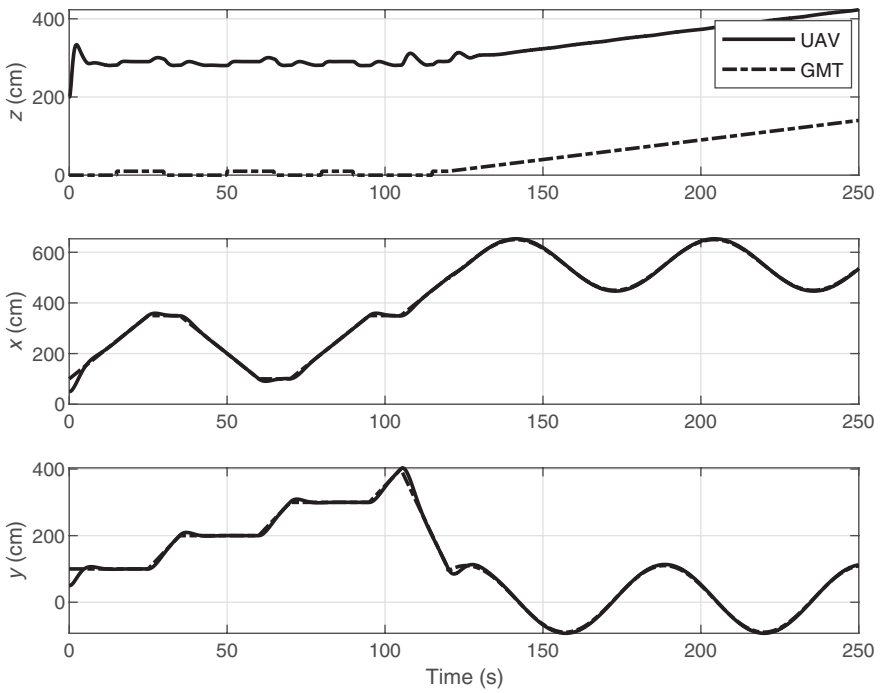

Figure 6. The components of the position of the UAV and the target over time.

simulation. This simulation evaluate the controller performance; however, the next simulation focuses on the guidance law, which should maintain the target in the FOV in the event of the controller errors. The 3D representation of GMT tracking is shown in Fig. 4, and its 2D representations are shown in Fig. 5. As can be seen, tracking and maintaining the moving target in the field of view has been done in various target manoeuver. Figure 6 shows the time history of the movement of the target and the UAV in x, y, and z directions. The tracking

https://doi.org/10.1017/aer.2021.23 Published online by Cambridge University Press

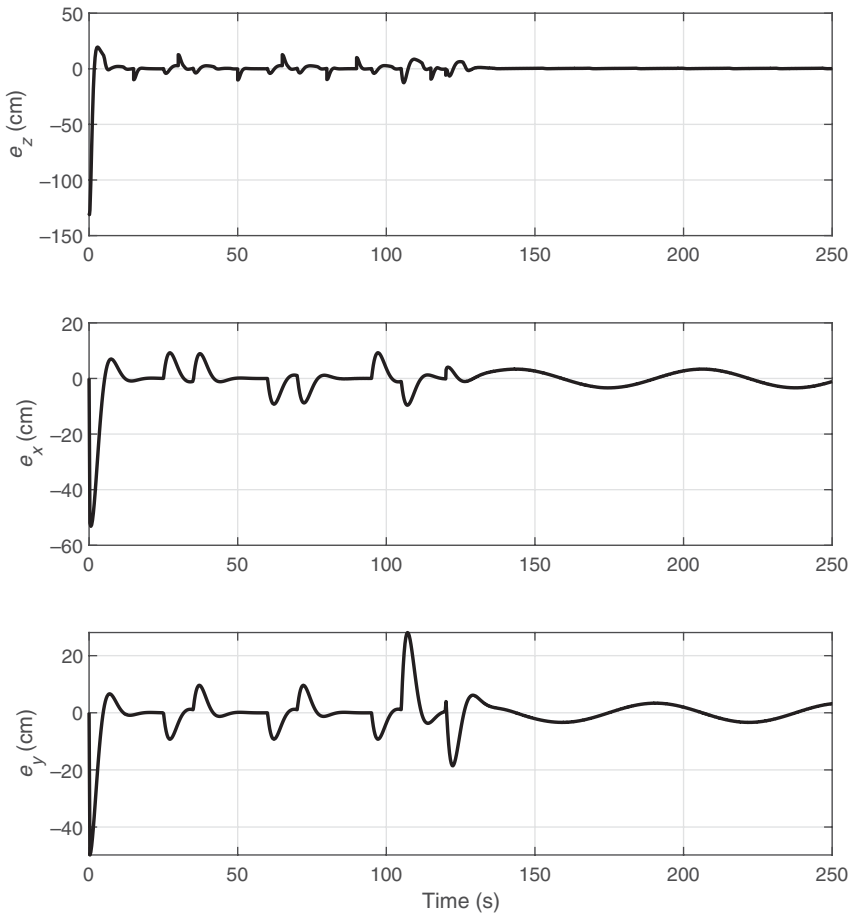

Figure 7. The components of the position tracking error by the UAV.

errors of the position and the attitude reference signals by the UAV are shown in Figs. 7 and 8, respectively. The jumps in the error signals are caused by sudden changes in the direction of the target trajectory. For example, at 25 and 35 seconds, the moving target changes its direction that causes jumps in the related error signals at the same time. Another reason for these error jumps are the wind turbulence. For example, in the e_ψ error signal, perturbation occurs at the 200 seconds which causes error jumps at the same moment. It should be noted that despite the perturbation remaining, the controller has removed its effect well. These figures show that the proposed controller has good performance in tracking the reference generated trajectory by the guidance law.

Corresponding control inputs in this simulation are shown in Fig. 9. These signals indicate the PWMs of four actuators of the quadrotor. As can be seen, the amplitude of the inputs did not exceed the admissible interval [0 1], i.e. the actuators didn't saturate. Figure 10 shows $\gamma = e_z + \epsilon$ is positive all over the simulation times. This means that Lemma 3 is satisfied during the tracking mission which guaranties the target preserving in the FOV. Figure 11 shows the parameters affecting the guidance law designed in accordance with Equation (20)

https://doi.org/10.1017/aer.2021.23 Published online by Cambridge University Press

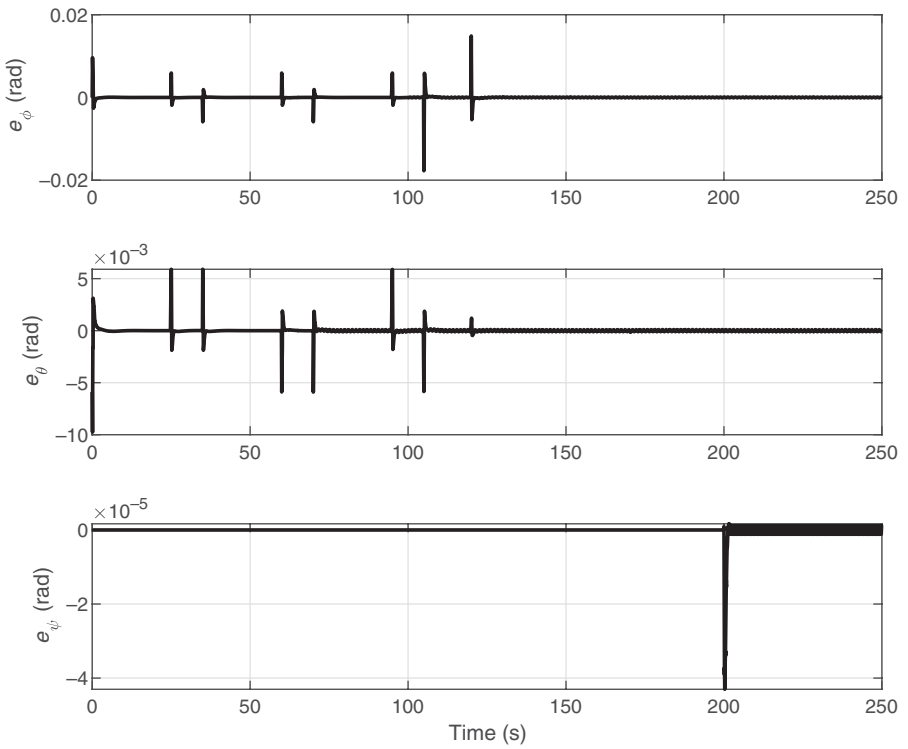

Figure 8. The components of the attitude tracking errors by the UAV.

in Lemma 3. It can be seen in this figure the relationship between the tracking errors on the $x-y$ plane, z_{mt}, the proposed desired altitude and the results of the desired altitude tracking.

Due to some unpredictable reasons in the real world, such as target acceleration estimation error, quadrotor actuator error, and etc., the quadrotor position deviates from the target. Figure 12 shows the the x and y components of the relative distance between the quadrotor and the target caused by the presence of acceleration estimation errors as $\delta_{a_z}^{mt} = 0.1\text{m/s}^2$, $\delta_{a_x}^{mt} = -0.5\text{m/s}^2$ and $\delta_{a_y}^{mt} = -0.4\text{m/s}^2$.

In such circumstances, in order to examine the characteristics of the proposed strategy in relation to existing researches, a comparison is made between two quadrotors called $Quad_1$ and $Quad_2$, in which the first quadrotor is equipped with the proposed guidance strategy and the second quadrotor is guided regardless of the altitude adjustment to hold the target.

For this purpose, γ and λ are defined as criterion parameters with the following form, which are defined according to the Lemmas 3 and 4, respectively;

$$\gamma = e_z(k) + \epsilon \qquad \text{with } z_r(k) = 2\max(|e_x|, |e_y|) + z_0(k)$$
$$\lambda = e_z(k) + \epsilon - 2\min(|e_x|, |e_y|) \qquad \text{with } z_r(k) = z_0(k)$$

According to Lemma 3, $\gamma(k) > 0$ ensures the target retention in the FOV during the tracking mission by the $Quad_1$ and regarding Lemma 4, $\lambda(k) < 0$ proves loss of target by the $Quad_2$.

https://doi.org/10.1017/aer.2021.23 Published online by Cambridge University Press

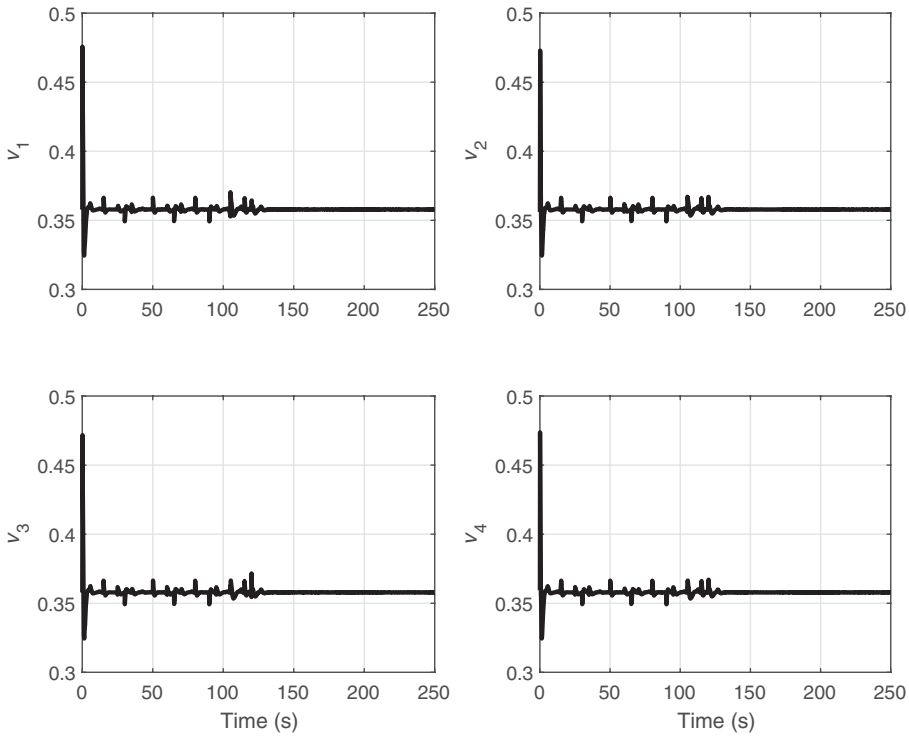

Figure 9. The control inputs of the quadrotor's actuators.

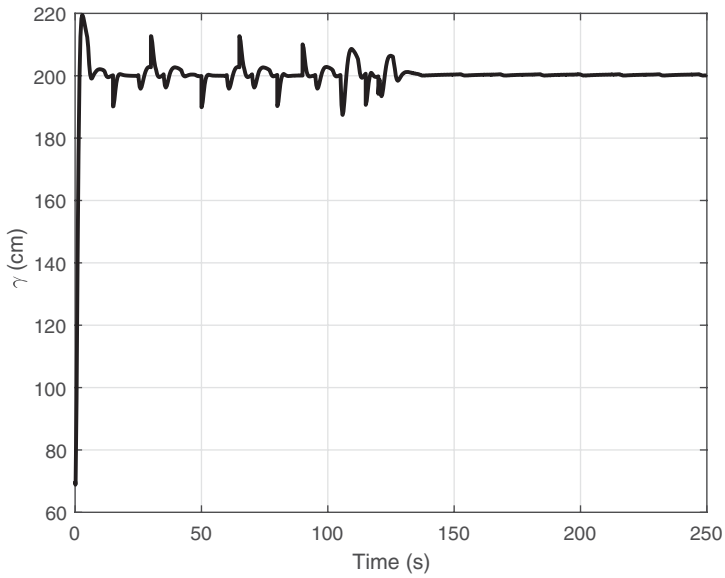

Figure 10. The sufficient condition parameter values.

https://doi.org/10.1017/aer.2021.23 Published online by Cambridge University Press

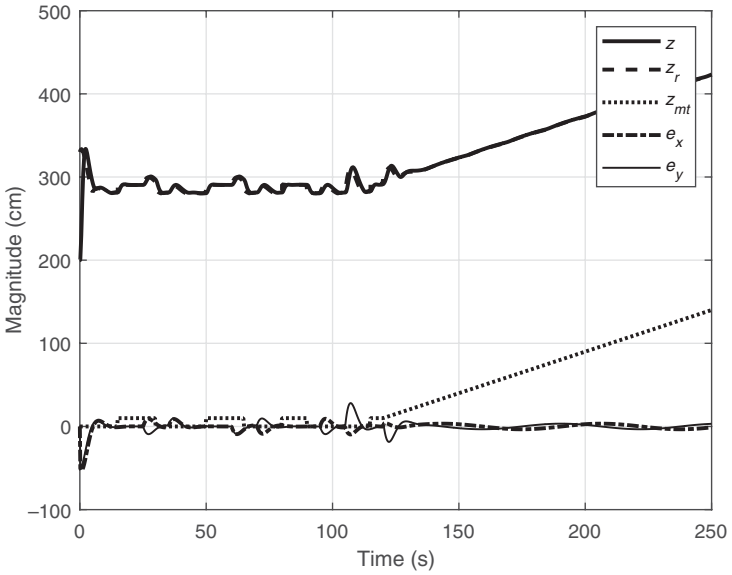

Figure 11. The parameters affecting the desired altitude calculation by the proposed guidance law.

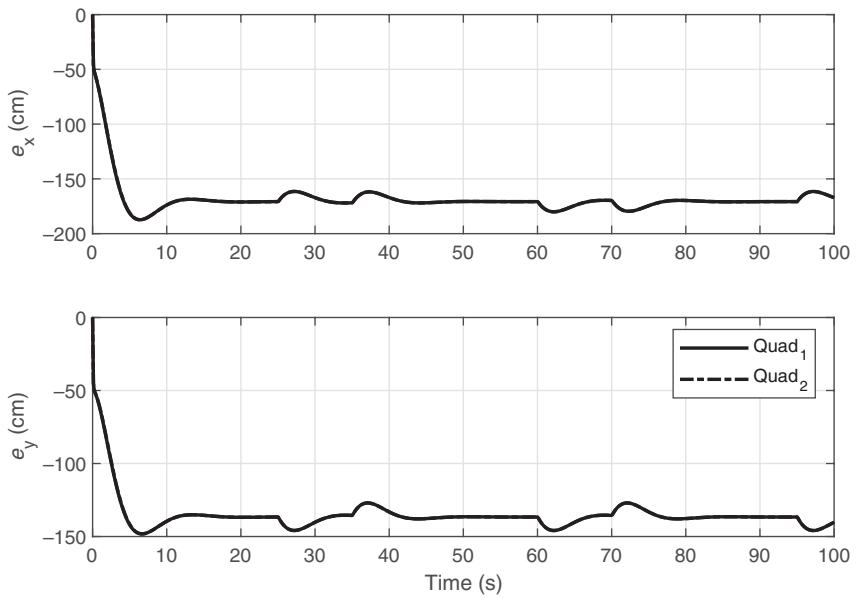

Figure 12. The *x* and *y* components of the relative distance between the quadrotor and the target.

As it is illustrated in Fig. 13, γ is positive during this simulation, which obtains the target retention in the FOV with $Qaud_1$. On the other hand, λ is negative, indicating the loss of target by $Quad_2$.

The desired altitude and their corresponding real values are illustrated in Fig. 14. As it can be seen, in contrast to $Quad_2$, the altitude of $Quad_1$ increases to provide the FOV needed to ensure the target is maintained.

https://doi.org/10.1017/aer.2021.23 Published online by Cambridge University Press

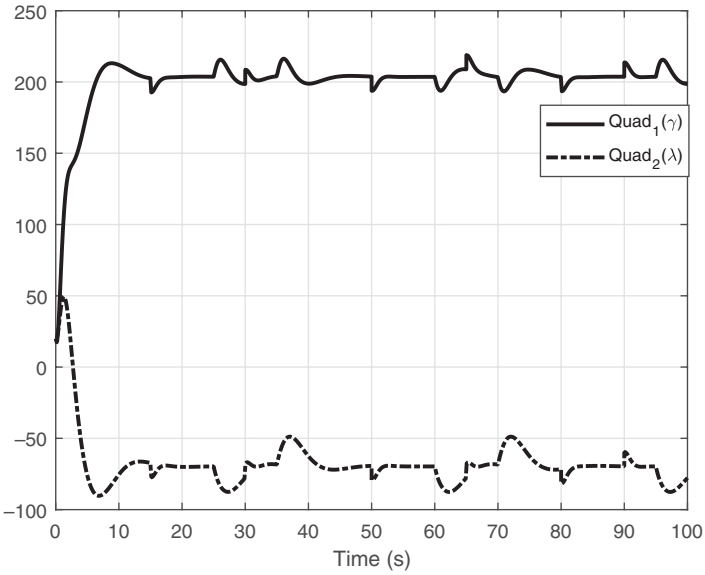

Figure 13. The values of the criterion parameters to guarantee the target preserving by Quad1 and the target missing by the Quad2.

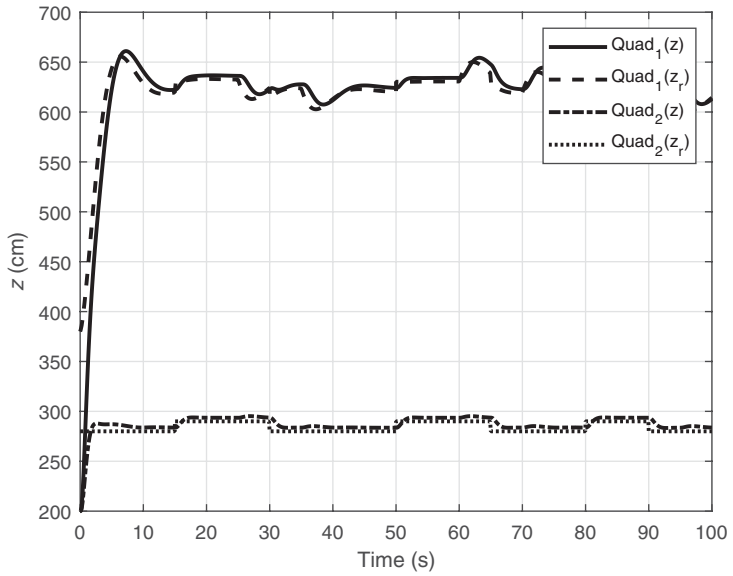

Figure 14. comparison between the reference altitudes of $Quad_1$ and $Quad_2$ and their tracking results.

6.0 CONCLUSION

In this paper, an aerial tracking guidance and control system is presented to preserve the ground moving target in the FOV. For this purpose, a reference altitude is generated for the quadrotor to provide the required FOV of the quadrotor, which consists of two critical and

https://doi.org/10.1017/aer.2021.23 Published online by Cambridge University Press

trusted regions. The dimensions of the trusted region are suggested as a function of the relative distance between the target and the quadrotor. Also, the dimensions of the critical region are determined according to the upper bounds of target localisation uncertainty and the quadrotor locations. In addition, the problem of temporal increase in the target velocity with respect to the quadrotor velocity is solved by considering larger dimensions for the critical region. Considering the desired dimensions of the regions, a sufficient condition is provided on the minimum altitude of the quadrotor, which ensures that the target is preserved in FOV despite the uncertainty of the target location and the changes in ground altitude. A MPC is employed to maintain the target at the center of the image and the desired altitude. Furthermore, the integral of the position error is used to achieve null steady-state error in the presence of the wind disturbances. It is shown analytically as well as by simulation that the proposed method ensures that the target is maintained in the FOV of the quadrotor in the presence of wind, quadrotor and target localisation uncertainty and terrain altitude variation. Future research includes evaluating the proposed method in the presence of a complete block of target localisation in which a complete of localisation error model used instead the maximum of the error. The altitude limit, which is influenced by the specifications of the quadrotor and its payload, should also be considered in proposing the guidance law. The use of cooperative UAVs is also one of possible solutions to reduce the flight altitude while preserving the target in the field of view. Practical implementation is another important activity that should be done in the future.

REFERENCES

1. GOMEZ-BALDERA, J.E., FLORES, G., CARRILLO, L.R.G. and LOZANO, R. Tracking a ground moving target with a quadrotor using switching control, *J. Intell. Robot. Syst.*, 2013, **70**, (1), pp 65–78.
2. GANS, N.R., NAGARAJAN, G., HU, K. and DIXON, W.E. Keeping multiple moving targets in the field of view of a mobile camera, *IEEE Trans. Rob.*, 2011, **27**, (4), pp 822–828.
3. ZHU, S., WANG, D. and LOW, C.B. Ground target tracking using UAV with input constraints, *J. Intell. Robot. Syst.*, 2012, **69**, pp 417–429.
4. KIM, D. and HONG, S.K. Target pointing and circling of a region of interest with quadcopter, *Int. J. Appl. Eng. Res.*, 2016, **11**, (2), pp 1082–1088.
5. ABBASI, E. and MAHJOOB, M. Quadrotor UAV guidance for ground moving target tracking, *J. Adv. Comput. Eng. Technol.*, 2016, **2**, (1), pp 37–44.
6. GHAMRY, K.A., DONG, Y., KAME, LM.A. and ZHANG, Y. Real-time autonomous take-off, tracking and landing of UAV on a moving UGV platform, 24th Mediterranean Conference on Control and Automation, 2016, pp 1236–1241.
7. ENGELHARDT, T., KONRAD, T., SCHAFER, B. and ABEL, D. Flatness-based control for a quadrotor camera helicopter using model predictive control trajectory generation, 24th Mediterranean Conference on Control and Automation, 2016, pp 852–859.
8. TAN, R. and KUMAR, M. Tracking of ground mobile targets by quadrotor unmanned aerial vehicles, *Unmanned Syst.*, 2014, **2**, pp 157–173.
9. PREVOST C., THERIAULT, O., DESBIENS, A., POULIN, E. and GAGNON, E. Receding horizon model-based predictive control for dynamic target tracking: a comparative study, AIAA Guidance, Navigation, and Control Conference, 2009, pp 62–68.
10. CHEN, J., LIU, T. and SHEN, S. Tracking a moving target in cluttered environments using a quadrotor, IEEE/RSJ International Conference on Intelligent Robots and Systems (IROS), 2016, pp 446–453.
11. KIM, S., OH, H. and TSOURDOS, A. Nonlinear model predictive coordinated standoff tracking of a moving ground vehicle, *J. Guidance Control Dyn.*, 2013, **36**, (2), pp 557–566.
12. OH, H., KIM, S., SHIN, H.S., WHITE, B.A., TSOURDOS, A. and RABBATH, A. Rendezvous and standoff target tracking guidance using differential geometry, *J. Intell. Rob. Syst.*, 2013, **69**, 389–405.

https://doi.org/10.1017/aer.2021.23 Published online by Cambridge University Press

13. LIU, X., YANG, Y., MA, C., LI, J. and ZHANG, S. Real-time visual tracking of moving targets using a low-cost unmanned aerial vehicle with a 3-axis stabilized gimbal system, *J. Appl. Sci.*, 2020, **10**, 5064. doi: 10.3390/app10155064.
14. YANG, X., ZHU, R., WANG, J. and LI, Z. Real-time object tracking via least squares transformation in spatial and Fourier domains for unmanned aerial vehicles, *Chin. J. Aeronaut.*, 2019, **32**, (7), pp 1716–1726.
15. DONG, F., YOU, K. and ZHANG, J. Flight control for UAV loitering over a ground target with unknown maneuver, *IEEE Trans. Control Syst. Technol.*, 2019, **28**, (6), 2461–2473.
16. LIANG, X., CHEN, G., ZHAO, S. and XIU, Y. Moving target tracking method for unmanned aerial vehicle/unmanned ground vehicle heterogeneous system based on AprilTag, *J. Meas. Control*, 2020, **53**, (3–4), pp 427–440.
17. ESPOSITO, N., FONTANA, U., D'AUTILIA , G. and BIANCHI, L. A hybrid approach to detection and tracking of unmanned aerial vehicles, *AIAA J.*, 2020. https://doi.org/10.2514/6.2020-1345.
18. COSTELO, M.F. Theory of the Analysis of Rotorcraft Operation in Atmospheric Turbulence, PhD thesis, Aerospace Engineering, Georgia Institute of Technology, Atlanta, GA, May 1992.
19. RAFFO, G.V., ORTEGA, M.G. and RUBIO, F.R. An integral predictive/nonlinear control structure for a quadrotor helicopter, *Automatica*, 2010, **46**, pp 29–39.
20. YANG, X., POTA, H. and GARRATT, M. Design of a gust-attenuation controller for landing operations of un-manned autonomous helicopters, 2009 *IEEE Control Applications*, (CCA) Intelligent Control, (ISIC), 2009, pp. 1300–1305.
21. PFLIMLIN, J.M., SOUERES, P. and HAMEL, T. Position control of a ducted fan VTOL UAV in crosswind, *Int. J. Control*, 2007, **80**, 666–683.
22. CHEVIRON, T., PLESTAN, F. and CHRIETTE, A. Position control of a ducted fan VTOL UAV in crosswind, *Int. J. Control*, 2009, **82**, pp 2206–2220.
23. WASLANDER, S., HOFFMANN, G., JANG, J.S. and TOMLIN, C. Multi-agent quadrotor testbed control design: integral sliding mode vs. reinforcement learning, IEEE/RSJ International Conference on Intelligent Robots and Systems, 2005. (IROS 2005), 2005, pp 3712–3717.
24. ALEXIS, K., NIKOLAKOPOULOS, G. and TZES, A. On trajectory tracking model predictive control of an unmanned quadrotor helicopter subject to aerodynamic disturbances, *Asian. J. Control*, 2014, **16**, pp 209–224.
25. BOUABDALLAH, S. and SIEGWART, R. Full control of a quadrotor, IEEE/RSJ International Conference on Intelligent Robots and Systems, 2007. IROS 2007, 2007, pp 153–158.
26. SUNAN, T.K.K.H. and HENG, L.T. *Applied Predictive Control*, Springer-Verlag, 2002, New York, ch 3.
27. CAMACHO, E. and BORDONS, C. *Model Predictive Control*, Springer-Verlag, 2007, New York, ch 2.

https://doi.org/10.1017/aer.2021.23 Published online by Cambridge University Press